The Influence of Communication Bandwidth on Target Tracking with Angle Only Measurements from Two Platforms

Branko Ristic and
Sanjeev Arulampalam

DSTO-TR-1053

20010110 015

The Influence of Communication Bandwidth on Target Tracking with Angle Only Measurements from Two Platforms

Branko Ristic and Sanjeev Arulampalam

Surveillance Systems Division
Electronics and Surveillance Research Laboratory

DSTO–TR–1053

ABSTRACT

A multi-platform angle-only tracking system combines the angular measurements from distributed networked sensors in order to estimate the full kinematic target state. This report investigates the effect of communication bandwidth on track quality in a system which receives angle-only measurements from two networked sensors installed on two airborne moving platforms. The investigation is based on the Cramér-Rao lower bound of the mean-square range error for the case considered. The bound is derived for recursive estimators with prior information and compared with two algorithms: (i) maximum likelihood estimation over a cumulative measurement set and (ii) extended Kalman filter with triangulated range estimates.

APPROVED FOR PUBLIC RELEASE

DEPARTMENT OF DEFENCE
DEFENCE SCIENCE & TECHNOLOGY ORGANISATION
DSTO

DTIC QUALITY INSPECTED 3

APPROVED FOR PUBLIC RELEASE

The Influence of Communication Bandwidth on Target Tracking with Angle Only Measurements from Two Platforms

EXECUTIVE SUMMARY

Tracking targets using line-of-sight angular measurements is very important for tactical air surveillance. One reason is that passive sensors (such as the ESM receiver, Infrared Search and Track sensors or the radar in a passive mode), which enable covert mode operation, provide only the target angular measurements. However, even the use of an active sensor such as the radar, in the presence of Electronic Counter Measures (noise or deceptive jamming) provides reliably only the measurements of the target line-of-sight angle.

The aim of a multi-platform angle-only tracking system is to combine the angular measurements from (possibly moving) distributed networked sensors in order to estimate the full kinematic target state (including range, speed and heading). The quality of target tracking is obviously going to be influenced by the amount of information that is exchanged between the networked sensors. In practical systems this amount of information is limited by the capacity of the communication link or its bandwidth.

This report investigates the effect of bandwidth on the track quality in a system which receives angle-only measurements from two networked sensors installed on two airborne moving platforms. The method of investigation is based on the Cramér-Rao lower bounds which are derived for recursive estimators with prior information. As expected the tracking performance in the limited bandwidth environment is between the two extremes, the full-connection and the no-connection cases, and it follows the pattern of the received measurements over the link. As time progresses, the limited (but non-zero) bandwidth cases tend to approach the full connection performance. This effect is more pronounced when angular accuracy is higher.

The analysis shows that only relatively modest communication bandwidth, well within the capacity of modern data-links such as Link-16, is required for the target state estimate to rapidly approach the limit posed by the Cramér-Rao bound. Thus it appears that netting of angle-only information could provide considerable tactical advantage in resolving target position, heading and speed even in the presence of ECMs. Further investigation of this research area is warranted with an aim to relax some of the assumptions made in this analysis.

Authors

Branko Ristic
Surveillance Systems Division

Branko Ristic received his first two degrees in Yugoslavia: BEng from the University of Novi Sad in 1984 and MSc from The Belgrade University in 1991 (both in Electrical Engineering). He received the PhD degree from the Signal Processing Research Centre at Queensland University of Technology (QUT) in 1995. Between 1984 and 1989 he was a research engineer in the Vinca Institute in Belgrade. In February 1989 he arrived in Australia and became a senior research assistant at The University of Queensland (1989-1991) and QUT (1991-1993), senior DSP engineer in GEC Marconi Systems (1995) and Research Fellow at QUT (1996). In May 1996 he joined DSTO where he was initially working on enhancements to the Jindalee tracker. He is currently a Senior Research Scientist responsible for tracking and multi-sensor integration on airborne platforms. His main research interests include target tracking, estimation and nonlinear filtering.

Sanjeev Arulampalam
Surveillance Systems Division

Sanjeev Arulampalam received the B.Sc degree in Mathematical Sciences and the B.E degree with first class honours in Electrical and Electronic Engineering from the University of Adelaide in 1991 and 1992, respectively. In 1992 he joined the staff of Computer Sciences of Australia (CSA) where he worked as a Software Engineer in the Safety Critical Software Systems group. At CSA he was responsible for undertaking a hazard analysis on a computerised train control system. In 1993, he won a Telstra Postgraduate Fellowship award to work toward a Ph.D degree in Electrical and Electronic Engineering at the University of Melbourne, which he completed in 1997. His doctoral dissertation was "Performance Analysis of Hidden Markov Model based Tracking Algorithms". Upon completion of his postgraduate studies, Dr Arulampalam joined DSTO in 1998 as a Research Scientist. Since then he has worked on tender evaluation of the AEW&C contracts, and is currently involved in angle-only target motion analysis research for the F/A-18 project. His research interests include estimation theory, signal processing, and target motion analysis.

Contents

Figures

Glossary

CRLB Cramér-Rao lower bound

EKF Extended Kalman filter

FIM Fisher Information Matrix

MLE Maximum Likelihood estimation

1   Introduction

Modern tactical surveillance systems increasingly tend to operate in a covert mode using passive instead of active sensors. For air surveillance typical passive sensors include ESM receivers, Infrared Search and Track sensors and the radar in a passive mode. The main disadvantage of passive sensors, however, is that they are unable to measure target range; they provide only target angular measurements.

The aim of multi-platform angle-only tracking system is to combine the angular measurements from (possibly moving) distributed networked sensors in order to estimate the full kinematic target state (from which one can then work out the range, heading, speed). The single platform case has been studied in numerous publications, some more recent ones being [1], [3, Ch.5], [4]. It is well known that in the single observer case the ownship must "outmanoeuvre" the target in order to estimate the full target kinematic state [5]. In the multi-platform case the ownship manoeuvre is not necessary (providing the vergence angle is large enough) but the quality of target tracking is influenced by the amount of information that is exchanged between the networked sensors. In practical systems this amount of information is limited by the available capacity (or bandwidth) of the tactical data link used for communication.

This report investigates the effect of bandwidth on the track quality in a system which receives angle-only measurements from two networked sensors installed on two airborne moving platforms. The investigation is based on the study of the Cramér-Rao lower bound (CRLB) which defines the best achievable performance. The CRLB in the case considered is shown to depend on the observer-target geometry, the angular measurement accuracy, the sampling interval and the bandwidth. The report follows the style and extends the results recently reported in [4]. The bound is derived for recursive estimators with prior information and compared with two algorithms: (i) maximum likelihood estimation over a cumulative measurement set and (ii) extended Kalman filter with triangulated range estimates. In order to make the analysis tractable the following assumptions are made in the report: measurements are collected synchronously on both platforms with a unity probability of detection and with no false alarms; only a single non-manoeuvering target is being tracked; there are no registration errors and there is no transmission delay.

The report is organised as follows. Section 2 defines the problem of angle-only tracking with two communicating airborne platforms. Section 3 derives the Cramér-Rao lower bounds for the described problems. The influence of bandwidth on tracking performance is studied in Section 4, using the derived Cramér-Rao bounds. This section also compares two tracking algorithms against the bounds. Section 5 summarises the main results of the report.

2   Problem Description

Target T in Figure 1 is moving with a constant velocity along a straight line in x-y plane, while two friendly platforms P_1 and P_2, connected by a tactical data link, are collecting angular (azimuthal) measurements $z_1(k)$ and $z_2(k)$ respectively at time instances $t_k = kT_o$, $k = 1, \ldots, N$. Here T_o is the sampling interval while N is the number of

measurements. Azimuth measurements are defined with respect to the y axis direction and are affected by additive noise, i.e.

$$z_m(k) = \arctan \frac{x_t(k) - x_m(k)}{y_t(k) - y_m(k)} + w_m(k) \qquad (m = 1, 2) \tag{1}$$

where $\{x_t(k), y_t(k)\}$ are the unknown target coordinates and $\{x_m(k), y_m(k)\}$ are the known coordinates of sensors $m = 1, 2$. Noise processes $w_1(k)$ and $w_2(k)$ are mutually uncorrelated zero-mean white Gaussian with variances σ_1^2 and σ_2^2 respectively, i.e. $w_m \sim \mathcal{N}(0, \sigma_m^2)$. The target motion is assumed to be purely deterministic, i.e. there is no process noise involved.
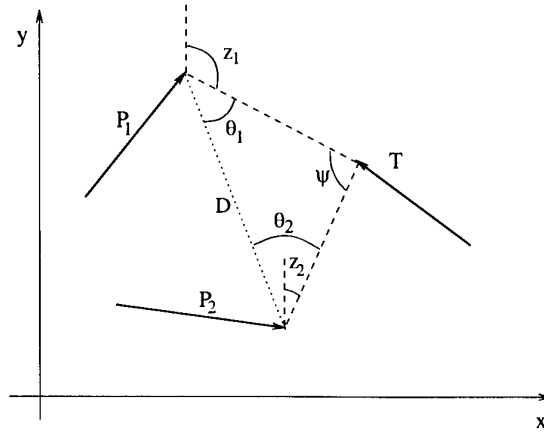

Figure 1: Trajectories of friendly platforms (P_1, P_2) and target T; z_1 and z_2 represent angular measurements, ψ is the vergence angle

Assume that identical angle-only trackers are placed on each of the friendly platforms. Then we may consider just one of them, for example the one on platform 1. The simple architecture is shown in Figure 2. The local sensor is sending angular measurements $z_1(k)$ at every sampling instant t_k. The on-board inertial navigation system (INS) is supplying the own-ship state vector[1] $s_1(k) = [x_1(k), \dot{x}_1(k), y_1(k), \dot{y}_1(k)]^T$ at the same time. Occasionally, at time instants $t_l = l T_o$ where $l = b + \eta k$, the tracker receives via the communication link additional angular measurements $z_2(l)$ and own-ship state vector $s_2(l)$ from the other platform. The assumption is that both $s_1(k)$ and $s_2(l)$ are known exactly. Parameter $b = 0, 1, 2, \ldots$ defines the delay in the initial measurement transmission while $\eta = 1, 2, 3, \ldots$ is a function of bandwidth. The case $b = 0$, $\eta = 1$ corresponds to the full connection scheme, where all measurements are exchanged instantaneously between the platforms. The case $b > N$ represents the opposite single-observer or no-link situation, studied for instance in [4]. Cases $\eta = 2, 3$, etc. represent the cases where only every second, third, etc. measurement is sent over the link. The relationship between the bandwidth B and parameter η is straightforward:

$$B = \frac{N_b}{\eta T_o} \tag{2}$$

---

[1]Vectors are represented by boldface lower case letters.

where N_b is the total number of bits per message[2]. Given a link with a specified bandwidth B_o, parameter η can be calculated as:

$$\eta = \lceil \frac{N_b}{B_o T_o} \rceil. \tag{3}$$

Next we investigate the influence of the tactical data link bandwidth on angle-only tracking accuracy.
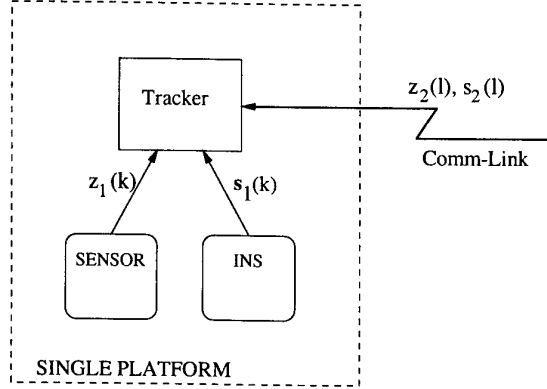

Figure 2: Tracking architecture

3   Cramér-Rao bound

Taking into account that the target is travelling at a *constant* velocity along a straight line, the unknown target state vector can be represented as a function of time index $k = 1, \ldots, N$ as follows:

$$\mathbf{s}(k) = [s_1(k) \ \ s_2(k) \ \ s_3(k) \ \ s_4(k)]^T = [x_t(k) \ \ \dot{x}_t \ \ y_t(k) \ \ \dot{y}_t]^T. \tag{4}$$

The covariance matrix of the unbiased estimator $\hat{\mathbf{s}}(k)$ is bounded by the inverse of the Fisher Information matrix[3] (FIM) $\mathbf{J}$:

$$\mathrm{E}\{([\hat{\mathbf{s}}(k) - \mathbf{s}(k)][\hat{\mathbf{s}}(k) - \mathbf{s}(k)]^T\} \geq \mathbf{J}^{-1}(k) \tag{5}$$

The FIM is defined as[4] [9]:

$$\mathbf{J}(\mathbf{s}) = \mathrm{E}\{[\bigtriangledown_{\mathbf{s}} \log p(Z, \mathbf{s})] [\bigtriangledown_{\mathbf{s}} \log p(Z, \mathbf{s})]^T\} \tag{6}$$

where Z is the cumulative measurement set which represents a union

$$Z = Z_1 \cup Z_2. \tag{7}$$

---

[2]A message from platform m typically would consists of a triple $\{z_m(t_l); \mathbf{s}_m(t_l); t_l\}$

[3]Matrices are represented by upper case boldface letters.

[4]In order to simplify notation we drop out index k unless there is possible confusion.

Measurements Z_1 are from platform P_1 and measurements Z_2 are from platform P_2, and at time index k they can be expressed as:

$$
\begin{aligned}
Z_1(k) &= \{z_1(i); i = 1, \ldots, k\} \\
Z_2(k) &= \{z_2(j); j = 1 + b + \eta l; \ l = 0, \ldots, \lceil \frac{k}{\eta} \rceil - b - 1\}
\end{aligned}
\tag{8}
$$

Density $p(Z, \mathbf{s})$ in (6) is a joint measurement-state probability density function. Note that in our model (described in Section 2) both measurements and target state are random. The target state $\mathbf{s}$ is random despite the assumption of the deterministic evolution of the target state (i.e. no process noise), because the initial target state $\mathbf{s}(0)$ is assumed to be random. The expectation operator E{ } in (6) is taken with respect to both Z and $\mathbf{s}$. Finally, $\nabla_\mathbf{s}$ in (6) is the gradient operator with respect to $\mathbf{s}$.

3.1   The Joint Measurement-State Density

Due to the independence between measurements[5] Z_1 and Z_2, the joint measurement-state density function $p(Z, \mathbf{s})$ can be expressed at time index k as follows:

$$
\begin{aligned}
p[Z(k), \mathbf{s}(k)] &= p[\mathbf{s}(k)] \cdot p[Z(k)|\mathbf{s}(k)] \\
&= p[\mathbf{s}(k)] \cdot p[Z_1(k)|\mathbf{s}(k)] \cdot p[Z_2(k)|\mathbf{s}(k)].
\end{aligned}
\tag{9}
$$

Probability density $p[\mathbf{s}(k)]$ represents the prior density of the target state which is either known or can be worked out using the prior information about the sensor and the target. Typically one knows the minimum and maximum sensor range, $r_{\min}$ and $r_{\max}$, respectively, as well as the maximum target speed $v_{\max}$. The common approach is to assume a Gaussian prior density at $k = 0$, that is, $\mathbf{s}(0) \sim \mathcal{N}(\mathbf{s}_0, \mathbf{P}_0)$. The prior density is then:

$$
p[\mathbf{s}(0)] = \frac{1}{(2\pi)^2 \sqrt{|\mathbf{P}_0|}} \exp\left\{-\frac{1}{2}(\mathbf{s} - \mathbf{s}_0)^T \mathbf{P}_0^{-1} (\mathbf{s} - \mathbf{s}_0)\right\}.
\tag{10}
$$

The mean of density $p[\mathbf{s}(0)]$, denoted as $\mathbf{s}_0$, is either a priori known or is calculated using the previous (at $k = 0$) angular measurement $z_1(0)$:

$$
\mathbf{s}_0 = [\bar{r} \sin z_1(0) + x_1(0), \quad 0, \quad \bar{r} \cos z_1(0) + y_1(0), \quad 0]^T,
\tag{11}
$$

where $\bar{r} = (r_{\max} + r_{\min})/2$ and $\mathbf{s}_1(0)$ is the platform 1 own-ship state vector at $k = 0$. The covariance of $p[\mathbf{s}(0)]$ is typically

$$
\mathbf{P}_0 = \mathrm{diag}(\sigma_r^2, \sigma_v^2, \sigma_r^2, \sigma_v^2)
\tag{12}
$$

where σ_r and σ_v are chosen in such a way that the prior density covers the entire span of the target range (from $r_{\min}$ to $r_{\max}$) and velocity (from $-v_{\max}$ to $+v_{\max}$). Next we need to work out the contribution of the prior density at time index k. Note that due to the purely deterministic target motion the following linear relationship holds:

$$
\mathbf{s}(k) = \mathbf{F}^k \mathbf{s}(0)
\tag{13}
$$

---

[5]The independence of the measurements is due to the independence of the measurement noise on the platforms.

where

$$\mathbf{F} = \begin{bmatrix} 1 & T_o & 0 & 0 \\ 0 & 1 & 0 & 0 \\ 0 & 0 & 1 & T_o \\ 0 & 0 & 0 & 1 \end{bmatrix}, \qquad \mathbf{F}^k = \begin{bmatrix} 1 & kT_o & 0 & 0 \\ 0 & 1 & 0 & 0 \\ 0 & 0 & 1 & kT_o \\ 0 & 0 & 0 & 1 \end{bmatrix}. \tag{14}$$

Then it follows (see for instance [7, Theorem 2.11]) that $\mathbf{s}(k) \sim \mathcal{N}(\mathbf{s}_k, \mathbf{P}_k)$, where

$$\mathbf{s}_k = \mathbf{F}^k \mathbf{s}_0 \text{ and } \mathbf{P}_k = \mathbf{F}^k \mathbf{P}_0 [\mathbf{F}^k]^T. \tag{15}$$

In expression (9), $p[Z_1(k)|\mathbf{s}(k)]$ represents the likelihood function due to the own-ship measurements. Since measurement noise $w_1(k)$ in (1) is Gaussian,

$$p[Z_1(k)|\mathbf{s}(k)] = \prod_{i=1}^{k} \frac{1}{\sigma_1 \sqrt{2\pi}} \exp\left\{ -\frac{[z_1(i) - h_1(\mathbf{s}, i)]^2}{2\sigma_1^2} \right\} \tag{16}$$

where (keeping in mind eq.(4))

$$h_1(\mathbf{s}, i) = \arctan \frac{s_1(k) - (k-i)T_o\, s_2(k) - x_1(i)}{s_3(k) - (k-i)T_o\, s_4(k) - y_1(i)}. \tag{17}$$

Finally the third density term on the right-hand side of (9) is the likelihood function due to the measurements from platform 2. The same reasoning as above leads to the following expression:

$$p[Z_2(k)|\mathbf{s}(k)] = \prod_{i=(1+b):\eta}^{k} \frac{1}{\sigma_2 \sqrt{2\pi}} \exp\left\{ -\frac{[z_2(i) - h_2(\mathbf{s}, i)]^2}{2\sigma_2^2} \right\} \tag{18}$$

where notation $i = (1 + b) : \eta$ signifies that η is the increment (i.e. index i takes the values $1 + b, 1 + b + \eta, 1 + b + 2\eta, \dots$). Similarly to (17) we have

$$h_2(\mathbf{s}, i) = \arctan \frac{s_1(k) - (k-i)T_o\, s_2(k) - x_2(i)}{s_3(k) - (k-i)T_o\, s_4(k) - y_2(i)}. \tag{19}$$

Note. The expression for the joint density function (9) could be generalised in a straightforward manner to the case of three or more platforms by adding the appropriate likelihood functions in the product.

3.2 Fisher Information Matrix

Before calculating the FIM of eq.(6) let us consider the negative logarithm of $p(Z, \mathbf{s})$,

$$\lambda(Z, \mathbf{s}) = -\log p(Z, \mathbf{s})$$

$$= C + \frac{1}{2}(\mathbf{s} - \mathbf{s}_k)^T \mathbf{P}_k^{-1} (\mathbf{s} - \mathbf{s}_k) + \frac{1}{2\sigma_1^2} \sum_{i=1}^{k} [z_1(i) - h_1(\mathbf{s}, i)]^2$$

$$+ \frac{1}{2\sigma_2^2} \sum_{j=1+b:\eta}^{k} [z_2(j) - h_2(\mathbf{s}, j)]^2 \tag{20}$$

where C denotes a constant. In a shortened notation (20) can be expressed as:

$$\lambda(Z, \mathbf{s}) = C + \lambda_0(\mathbf{s}) + \lambda_1(Z_1, \mathbf{s}) + \lambda_2(Z_2, \mathbf{s}). \qquad (21)$$

From the definition of the FIM in (6) we have:

$$\mathbf{J}(\mathbf{s}) = \mathrm{E}\{[\nabla_\mathbf{s}(C + \lambda_0 + \lambda_1 + \lambda_2)] \, [\nabla_\mathbf{s}(C + \lambda_0 + \lambda_1 + \lambda_2)]^T\} \qquad (22)$$

Using the linearity of the gradient operator and the mutual independence of Z_1, Z_2 and $\mathbf{s}(0)$, we can write

$$\mathbf{J} = \mathbf{J}_0 + \mathbf{J}_1 + \mathbf{J}_2 \qquad (23)$$

where

$$\mathbf{J}_m = \mathrm{E}\{[\nabla_\mathbf{s}\lambda_m][\nabla_\mathbf{s}\lambda_m]^T\} \qquad (m = 0, 1, 2)$$

Next we derive each term in (23).

3.2.1 Derivation of $\mathbf{J}_0$.

Note that [6]

$$\nabla_\mathbf{s}\lambda_0(\mathbf{s}) = \frac{1}{2}\frac{\partial[(\mathbf{s} - \mathbf{s}_k)^T \mathbf{P}_k^{-1}(\mathbf{s} - \mathbf{s}_k)]}{\partial \mathbf{s}} = \mathbf{P}_k^{-1}(\mathbf{s} - \mathbf{s}_k) \qquad (24)$$

Then using the basic rules of matrix algebra and the fact that the inverse of the covariance matrix is a symmetric matrix we have

$$\begin{aligned}
\mathbf{J}_0 &= \mathrm{E}\{\mathbf{P}_k^{-1}(\mathbf{s} - \mathbf{s}_k)((\mathbf{s} - \mathbf{s}_k)^T[\mathbf{P}_k^{-1}]^T\} \\
&= \mathbf{P}_k^{-1}\mathrm{E}\{(\mathbf{s} - \mathbf{s}_k)((\mathbf{s} - \mathbf{s}_k)^T\}\mathbf{P}_k^{-1} \\
&= \mathbf{P}_k^{-1}\,\mathbf{P}_k\,\mathbf{P}_k^{-1} = \mathbf{P}_k^{-1}
\end{aligned} \qquad (25)$$

3.2.2 Derivation of $\mathbf{J}_1$ and $\mathbf{J}_2$.

From [4] it follows that:

$$\mathbf{J}_1 = \mathrm{E}\left\{\frac{1}{\sigma_1^2}\sum_{i=1}^{k}[\nabla_\mathbf{s}h_1(\mathbf{s}, i)] \, [\nabla_\mathbf{s}h_1(\mathbf{s}, i)]^T\right\} \qquad (26)$$

and

$$\mathbf{J}_2 = \mathrm{E}\left\{\frac{1}{\sigma_2^2}\sum_{i=1+b:\eta}^{k}[\nabla_\mathbf{s}h_2(\mathbf{s}, i)] \, [\nabla_\mathbf{s}h_2(\mathbf{s}, i)]^T\right\} \qquad (27)$$

where

$$\nabla_\mathbf{s}h_m = \begin{bmatrix} \dfrac{\partial h_m}{\partial s_1} & \dfrac{\partial h_m}{\partial s_2} & \dfrac{\partial h_m}{\partial s_3} & \dfrac{\partial h_m}{\partial s_4} \end{bmatrix}^T \qquad (m = 1, 2), \qquad (28)$$

and with expectation E in eqs.(26) and (27) taken over the prior distribution of **s**. The appropriate terms in (28) are as follows:

$$\frac{\partial h_m}{\partial s_1} = \frac{y_t(i) - y_m(i)}{[x_t(i) - x_m(i)]^2 + [y_t(i) - y_m(i)]^2}$$

$$\frac{\partial h_m}{\partial s_2} = -(k - i) T_o \frac{\partial h_m}{\partial s_1}$$

$$\frac{\partial h_m}{\partial s_3} = -\frac{x_t(i) - x_m(i)}{[x_t(i) - x_m(i)]^2 + [y_t(i) - y_m(i)]^2}$$

$$\frac{\partial h_m}{\partial s_4} = -(k - i) T_o \frac{\partial h_m}{\partial s_3}$$

Let us introduce the following notation for the *relative* state vectors:

$$\tilde{\mathbf{s}}_m = \mathbf{s} - \mathbf{s}_m = [\tilde{x}_m, \ \tilde{\dot{x}}_m, \ \tilde{y}_m, \ \tilde{\dot{y}}_m]^T \qquad (m = 1, 2) \tag{29}$$

Note that $\tilde{\mathbf{s}}_m(k) \sim \mathcal{N}(\mathbf{s}_k - \mathbf{s}_m(k), \mathbf{P}_k)$ where $\mathbf{s}_k$ and $\mathbf{P}_k$ were given by (15). It is now straightforward to verify that in order to evaluate the 4×4 matrices $\mathbf{J}_1$ and $\mathbf{J}_2$ we need to work out the expressions for

$$\mathrm{E}\left\{\frac{\tilde{x}^2}{(\tilde{x}^2 + \tilde{y}^2)^2}\right\} \text{ and } \mathrm{E}\left\{\frac{\tilde{x}\tilde{y}}{(\tilde{x}^2 + \tilde{y}^2)^2}\right\}$$

where $\tilde{x}$ and $\tilde{y}$ are both Gaussian and independent. This step can be performed by numerical integration or Monte Carlo averaging [8].

The FIM given by (23) depends on (i) the geometry of the scenario (the motion of the communicating platforms and the target); (ii) measurements accuracy (σ_1 and σ_2); (iii) sampling interval (T_o); (iv) communication bandwidth (η). The CRLBs are calculated as the diagonal elements of the inverse FIM, i.e.

$$\mathrm{CRLB}\{\hat{s}_j\} = [\mathbf{J}^{-1}]_{jj} \qquad (j = 1, 2, 3, 4) \tag{30}$$

where s_j, $j = 1, 2, 3, 4$ are expressed in the Cartesian coordinates, see eq.(4). In practice, however, it is often of more interest to consider the estimate of target *range* and its CR lower bound. This CRLB will be derived next.

3.3 CRLB for the Target Range Estimate

The target range is a non-linear function of the state vector **s**:

$$R_t(k) = \sqrt{x_t^2(k) + y_t^2(k)} = g[\mathbf{s}(k)] \tag{31}$$

According to [9, pg.83]

$$\mathrm{CRLB}(\hat{R}_t) = \sum_i \sum_j \frac{\partial g(\mathbf{s})}{\partial s_i} \left(\mathbf{J}^{-1}\right)_{ij} \frac{\partial g(\mathbf{s})}{\partial s_j} \tag{32}$$

The partial derivatives are as follows:

$$\frac{\partial g}{\partial s_1} = \frac{x_t}{\sqrt{x_t^2 + y_t^2}} \tag{33}$$

$$\frac{\partial g}{\partial s_2} = 0 \tag{34}$$

$$\frac{\partial g}{\partial s_3} = \frac{y_t}{\sqrt{x_t^2 + y_t^2}} \tag{35}$$

$$\frac{\partial g}{\partial s_4} = 0, \tag{36}$$

which leads to the following expression:

$$\text{CRLB}(\hat{R}_t) = \frac{x_t^2}{x_t^2 + y_t^2}\text{CRLB}(\hat{x}_t) + \frac{x_t y_t}{x_t^2 + y_t^2}\left[(\mathbf{J}^{-1})_{13} + (\mathbf{J}^{-1})_{31}\right] + \frac{y_t^2}{x_t^2 + y_t^2}\text{CRLB}(\hat{y}_t) \tag{37}$$

Note. If estimates $\hat{x}_t$ and $\hat{y}_t$ are efficient (meet their respective CRLBs) the estimate of range $\hat{R}_t = \sqrt{\hat{x}_t^2 + \hat{y}_t^2}$ may not be efficient because $g(\mathbf{s})$ is non-linear [9, pg.84].

The next section will discuss the influence of bandwidth on the tracking performance and in addition will compare two algorithms for two-platform angle only-tracking with the derived CRLB.

4   The Influence of Bandwidth

4.1   Discussion

Consider the scenario shown in Figure 3 for the discussion that follows. A pair of communicating platforms flies in parallel at a speed of 540 km/h with a mutual distance of approximately 6 km during the first half of the scenario ($k = 1, \ldots, 30$). Then platform 1 performs a sharp turn in order to increase the vergence angle, and thereafter both platforms again move at the constant speed and heading. Target T is moving eastwards at a speed of 790 km/h. The sampling interval is $T_o = 2$ sec.

Since the considered scenario (including the initial target state $\mathbf{s}(0)$) is purely deterministic, the calculation of the CRLBs can be somewhat simplified. The uncertainty about $\mathbf{s}(0)$ can still be expressed in terms of the prior covariance matrix $\mathbf{P}_0$, but there is no need to perform the expectation operation in eqs.(26) and (27). For the purpose of studying the influence of bandwidth this will be adequate.

The CRLBs of the range estimates as a function of time index k are shown in Figure 4 for $b = 0$ and $\eta = 1, 2, 4, 8, 16$ and no-link (single P_1 observer) case. The prior covariance matrix $\mathbf{P}_0$ of (12) is chosen with parameters

$$\sigma_r = 25 \text{ km} \quad \text{and} \quad \sigma_v = 1080 \text{ km/h}. \tag{38}$$

The assumed standard deviation of angular measurements is $\sigma_1 = \sigma_2 = 0.5^o$. Consider the first extreme, the 'no-link' case. Note that at $k = 1$ the CRLB is determined by the
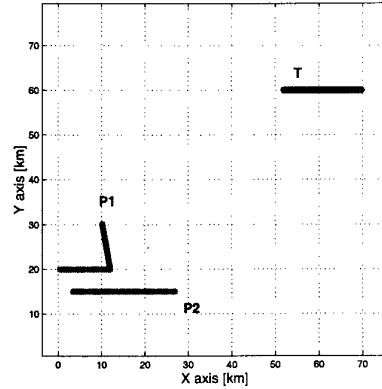
Figure 3: Angle-Only Tracking scenario

prior covariance matrix (the square root of the CRLB corresponds roughly to σ_r). As the time progresses the CRLB varies slightly due to the geometry and the collected angular measurements until the manoeuvre, when it sharply decreases as the target becomes "observable". The opposite extreme is the 'full connection' case ($\eta = 1$, $b = 0$). In this case the CRLB is significantly lower than in the 'no-link' case and completely independent of the manoeuvre as the target is observable throughout the scenario. The cases $\eta = 2, 4, 8, 16$ are between the two extremes, and the respective CRLBs follow the pattern of the received measurements over the communication link.

Consider for example the CRLB curve for $\eta = 16$ and $b = 0$ case in Figure 4. After receiving the first angle measurement from the other platform (at $k = 1$) the range estimate error standard deviation is about 12 km. Due to the lack of measurements for 16 consecutive time steps, the standard deviation will rise to the level which corresponds to the 'no-link' case (about 25 km). At $k = 17$ when the link becomes active again, the range error standard deviation drops dramatically , although not quite to the level which corresponds to the 'full-connection' case. Then it continues to rise again until the link is active again, etc. Interestingly, after the manoeuvre practically all $\eta = 2, 4, 8, 16$ cases converge to the full connection performance (after $k = 50$ their CRLBs are similar). For $b > 0$ the CRLBs are identical to the 'no-link' case for $1 \leq k < 1+b$. During the remaining interval $1 + b \leq k \leq N$, the CRLBs are identical to the $b = 0$ cases shown in Figure 4.

Figure 5 repeats the CRLBs of the range estimate errors, but this time the assumed measurement accuracy is 5 times better, i.e. $\sigma_1 = \sigma_2 = 0.1^o$. Notice that with the higher quality of angular measurements the need for a high capacity link is somewhat reduced, and the cases $\eta = 2$ or even $\eta = 4$ are almost as good as the full connection case.

4.2   Tracking Algorithms Against the CRLB

For completeness this section investigates the performance of a pair of algorithms for two-platform angle only tracking and compares their performance with the CRLBs derived and discussed earlier.
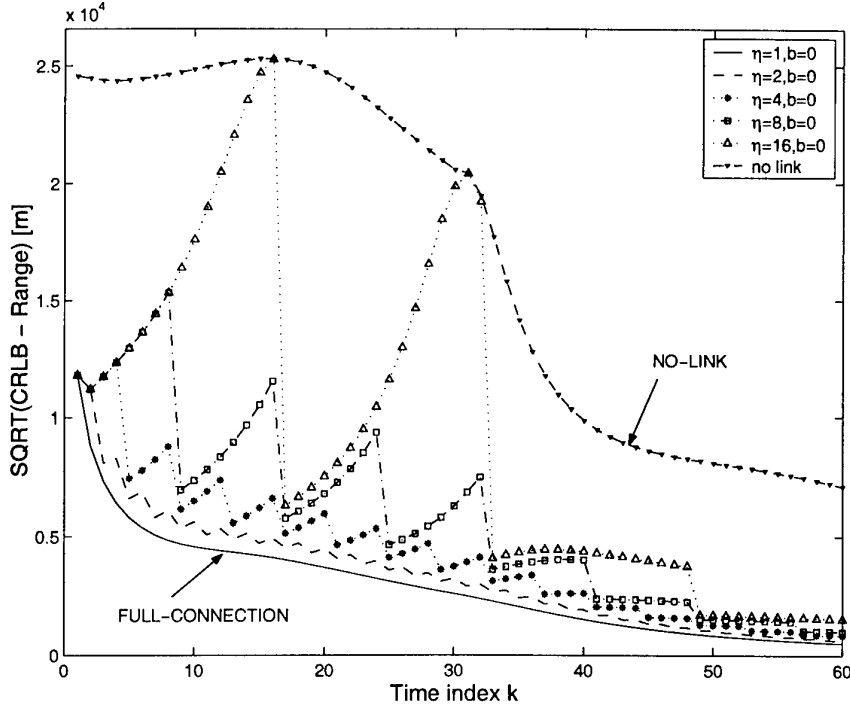
Figure 4: Cramér-Rao lower bounds of range estimate standard deviation for $\sigma_1 = \sigma_2 = 0.5^o$. The link parameters: $b = 0$ and $\eta = 1, 2, 4, 8, 16$ and no-link case.

4.2.1 MLE Algorithm

The first algorithm we consider is the Maximum Likelihood estimation (MLE) algorithm. We use MLE to estimate the range, keeping in mind the note made at the end of Section 3.3. The MLE is a batch algorithm although we are interested in the performance as a function of time index k. Hence we apply the MLE progressively at each time step, over a cumulative measurement set. The MLE implemented in this way is very close to an efficient estimator of range. Note however that MLE does not use prior information and hence is appropriate only for the "observable target" segments and larger values of k where the significance of prior information diminishes anyway. In mathematical terms the MLE is expressed as

$$\hat{\mathbf{s}}_{\mathrm{MLE}} = \arg\min_{\mathbf{s}} \lambda(\mathbf{s}) \tag{39}$$

where $\lambda(\mathbf{s})$ is given by (20). Minimisation was performed as in [4] using a MATLAB© routine *fmins*.

4.2.2 EKF with Triangulations

Next we consider a recursive algorithm which uses the prior information: an Extended Kalman filter (EKF) in the Cartesian coordinates with the use of triangulated range
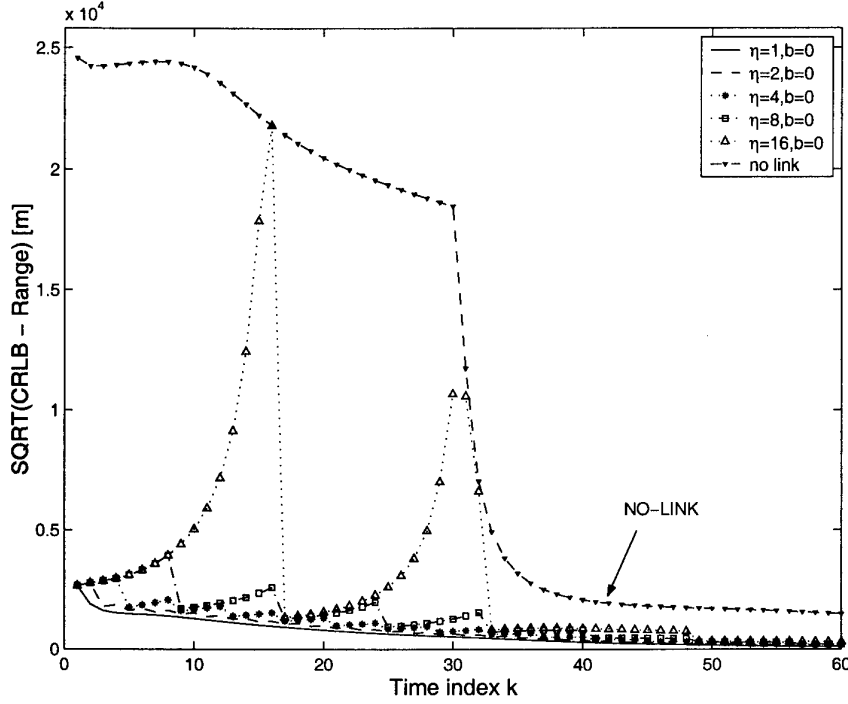
Figure 5: Cramér-Rao lower bounds of range estimate standard deviation for $\sigma_1 = \sigma_2 = 0.1^o$. The link parameters: $b = 0$ and $\eta = 1, 2, 4, 8, 16$ and no-link case.

estimates. This EKF is by the assumed convention (in relation to Figure 2.) installed on platform 1, and its measurement vector is defined as follows:

$$\mathbf{z}(k) = \begin{cases} z_1 & \text{if } k \neq l, \\ (\hat{R}_1, \ z_1)^T & \text{if } k = l. \end{cases} \tag{40}$$

Equation (40) indicates that when angular measurements from two platforms are available (if $k = l$) the measurement vector is augmented by the target range estimate (from platform 1) obtained by triangulation [3, Sec.10.6.4],

$$\hat{R}_1 = \frac{d \cdot \sin \theta_2}{\sin \psi}. \tag{41}$$

In order to explain eq.(41) we introduce unit vectors $\mathbf{u}_1$ and $\mathbf{u}_2$ defined as the directions from platform P_1 and P_2 respectively to target T (see Figure 1). They are calculated from measurements z_1 and z_2 as follows:

$$\mathbf{u}_m = \sin z_m \mathbf{i}_x + \cos z_m \mathbf{i}_y \qquad (m = 1, 2)$$

where $\mathbf{i}_x$ and $\mathbf{i}_y$ are unit vectors in the directions of the x and y axes, respectively. We also need to introduce the baseline vector $\mathbf{d}$ defined by the own-ship states $\mathbf{s}_1$ and $\mathbf{s}_2$ as: $\mathbf{d} = (x_2 - x_1)\mathbf{i}_x + (y_2 - y_1)\mathbf{i}_y$. Now the quantities in (41) are as follows: $d = |\mathbf{d}|$, $\psi = \arcsin(|\mathbf{u}_1 \times \mathbf{u}_2|)$ and $\theta_2 = \arcsin(|\mathbf{d} \times \mathbf{u}_2|/d)$. The variance of the triangulated range

11

is given by [3, Sec.10.6.4]

$$\sigma_{\hat{R}_1}^2 = \frac{\hat{R}_1^2 \, \cos^2 \psi \, \sigma_{\theta_1}^2 + \hat{R}_2^2 \sigma_{\theta_2}^2}{\sin^2 \psi} \tag{42}$$

where $\hat{R}_2 = d \cdot \sin\theta_1 / \sin\psi$, is the triangulated range from platform P_2. Since own-ship state vectors are known exactly, $\sigma_{\theta_1} = \sigma_1$ and $\sigma_{\theta_2} = \sigma_2$. Introducing the relative target state vector (with respect to platform 1) as in eq.(29),

$$\tilde{s}(k) = s(k) - s_1(k) = [\tilde{s}_1, \ \tilde{s}_2, \ \tilde{s}_3, \ \tilde{s}_4]^T$$

where $s(k)$ is the target state vector of eq.(4), the state equation can be expressed as follows:

$$\tilde{s}(k+1) = \mathbf{F} \, \tilde{s}(k) - \mathbf{U}(k+1, k) \tag{43}$$

where $\mathbf{F}$ was defined by (14) and

$$\mathbf{U}(k+1, k) = \begin{bmatrix} x_1(k+1) - x_1(k) - T_o \dot{x}_1(k) \\ \dot{x}_1(k+1) - \dot{x}_1(k) \\ y_1(k+1) - y_1(k) - T_o \dot{y}_1(k) \\ \dot{y}_1(k+1) - \dot{y}_1(k) \end{bmatrix}$$

is a vector of deterministic inputs which account for the observer (platform 1) acceleration. The measurement equation is non-linear,

$$\mathbf{z}(k) = h[\tilde{s}(k)] + \mathbf{w}(k). \tag{44}$$

The non-linear function $h[\ ]$ in (44) is defined as[6]:

$$h[\tilde{s}] = \begin{bmatrix} \sqrt{\tilde{s}_1^2 + \tilde{s}_3^2} \\ \arctan \frac{\tilde{s}_1}{\tilde{s}_3} \end{bmatrix}. \tag{45}$$

The covariance matrix of $\mathbf{w}(k)$ in (44) is $\mathbf{R} = \mathrm{diag}[\sigma_{\hat{R}_1}^2, \sigma_1^2]$, where $\sigma_{\hat{R}_1}^2$ is given by (42). The standard EKF equations [2, Sec.10.3.3] are applied with the equivalent measurement matrix given by:

$$\mathbf{H}_{k+1} = \frac{\partial h[\tilde{s}(k+1)]}{\partial \tilde{s}} \bigg|_{\tilde{s}=\hat{s}(k+1|k)} = \begin{bmatrix} \frac{\hat{s}_1}{\sqrt{\hat{s}_1^2+\hat{s}_3^2}} & 0 & \frac{\hat{s}_3}{\sqrt{\hat{s}_1^2+\hat{s}_3^2}} & 0 \\ \frac{\hat{s}_3}{\hat{s}_1^2+\hat{s}_3^2} & 0 & -\frac{\hat{s}_1}{\hat{s}_1^2+\hat{s}_3^2} & 0 \end{bmatrix}_{k+1|k} \tag{46}$$

4.2.3 Results

The simulations were performed for the scenario described in Section 4.1. The simulation results are shown in Figures 6.(a), (b) and (c) for cases (i) no-link (ii) $\eta = 8$, $b = 0$ and (iii) $\eta = 1$, $b = 0$ (full connection), respectively. In all cases the measurement noise was set to $\sigma_1 = \sigma_2 = 0.1°$, and the sampling interval was $T_o = 2$ sec. The y-axis in all

---

[6]We consider only $k = l$ case of (40), since the other one follows directly.

the figures represents the root-mean-square (RMS) range errors. The calculated CRLBs are always shown with dashed lines. The MLE curves are obtained from simulations by averaging over 100 independent Monte Carlo runs. As expected they match the calculated CRLBs. The EKF algorithm uses the prior knowledge about the target state in the form of the prior density (10). In the simulations the mean of the prior density was set to the true value of $s(0)$, while the covariance was the one used in the calculations of CRLBs [see (38)]. The EKF curves are obtained by averaging over 500 Monte Carlo runs, and are shown with dash-dotted lines with triangles. Since the EKF is a suboptimal algorithm, its RMS errors are always higher than the calculated CRLBs, although note that in all the cases considered they follow the trend of the respective bounds.

5   Summary

The influence of communication link bandwidth on angle-only tracking with a pair of communicating moving platforms is studied. The method of investigation is based on the Cramér-Rao lower bounds which are derived for recursive estimators with prior information. The bounds were confirmed by Monte Carlo simulations using the maximum likelihood estimator over a cumulative measurement set and the extended Kalman filter with triangulation. The tracking performance in the limited bandwidth environment is shown to be between the two extremes, the full-connection and the no-connection cases, and it follows the pattern of the received measurements over the link. As the time progresses the limited (but non-zero) bandwidth cases tend to approach the full connection performance. This effect is more pronounced when angular accuracy is higher.

The study presented in this report was carried out under a number of assumptions about: the target (non-manoeuvring single target), the sensor (no false detections and no missed detections) and the data link (no transmission delay). The future work will try to relax some of these assumptions.
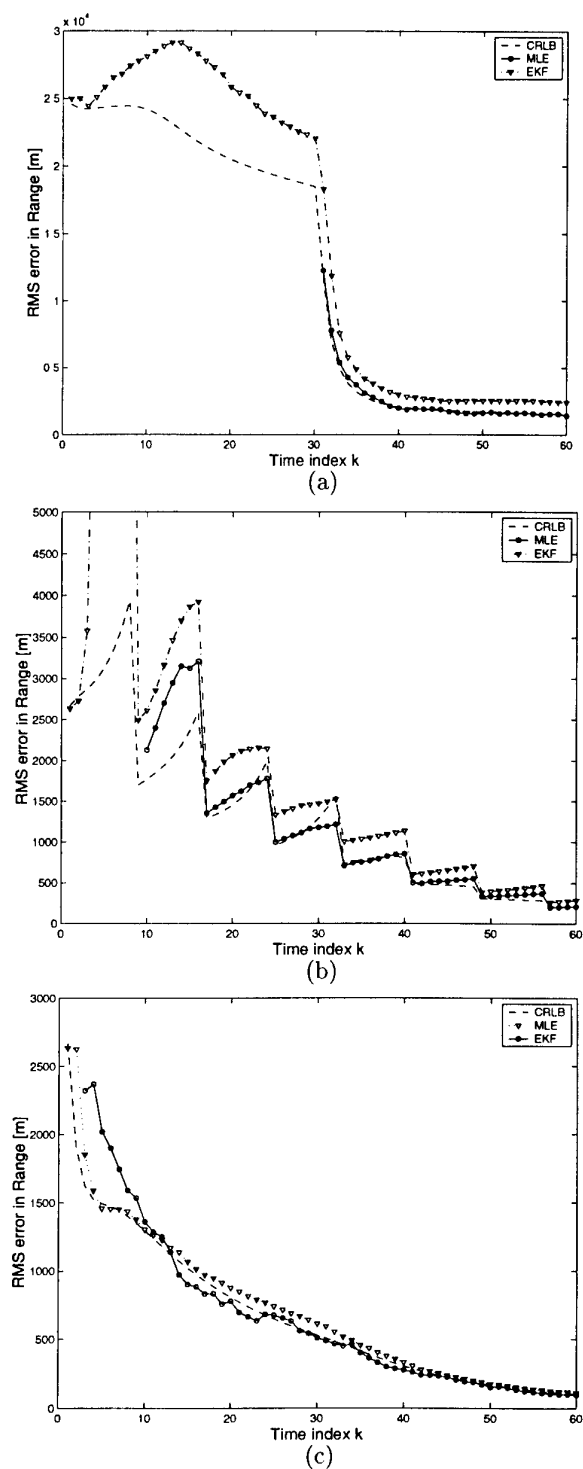
Figure 6: The RMS range errors of the MLE and the EKF+triangulation against the CRLBs. Simulations results for: (a) no-link case; (b) $\eta = 8$, $b = 0$ case; (c) $\eta = 1$, $b = 0$ (full connection) case.

References

1. Arulampalam, S. & Ristic, B. (2000) Comparison of the particle filter with range-parametrised and modified polar EKFs for angle-only tracking, *in Proc. of SPIE*, Vol. 4048, pp. 288–299.

2. Bar-Shalom, Y. & Li, X. R. (1993) *Estimation and Tracking*, Artech House.

3. Blackman, S. & Popoli, R. (1999) *Design and Analysis of Modern Tracking Systems*, Artech House.

4. Farina, A. (1999) Target tracking with bearings only measurements, *Signal Processing* **78**, 61–78.

5. Fogel, E. & Gavish, M. (1988) Nth-order dynamics target observability from angle measurements, *IEEE Trans. Aerospace and Electronic Systems* **AES-24**(3), 305–308.

6. Graybill, F. A. (1976) *Theory and Application of the linear model*, Duxbury Press, Belmont, CA.

7. Jazwinski, A. H. (1970) *Stochastic Processes and Filtering Theory*, Academic Press.

8. Ristic, B., Arulampalam, S. & Musso, C. (2000) On Cramer-Rao bounds for sequential angle-only target motion analysis, *in Proc. 3rd Australasian Workshop on Signal Processing Applications (WoSPA 2000)*, Brisbane, Australia.

9. VanTrees, H. L. (1968) *Detection, Estimation and Modulation Theory (Part I)*, John Wiley & Sons.

DISTRIBUTION LIST

The Influence of Communication Bandwidth on Target Tracking with Angle Only
Measurements from Two Platforms

Branko Ristic and Sanjeev Arulampalam

	Number of Copies
DEFENCE ORGANISATION	
Task Sponsor	
Gp Capt John Quaife,DACD	1
Gp Capt Clive Rossiter	1
S&T Program	
Chief Defence Scientist	
FAS Science Policy	1
AS Science Corporate Management	
Director General Science Policy Development	1
Counsellor, Defence Science, London	Doc Data Sht
Counsellor, Defence Science, Washington	Doc Data Sht
Scientific Adviser to MRDC, Thailand	Doc Data Sht
Scientific Adviser Policy and Command	1
Navy Scientific Adviser	Doc Data Sht
Scientific Adviser, Army	Doc Data Sht
Air Force Scientific Adviser	1
Director Trials	1
Aeronautical and Maritime Research Laboratory	
Director, Aeronautical and Maritime Research Laboratory	1
Chief, Weapons Systems Division	1
Chief, Maritime Operations Division	1
Dr David Kershaw, Head Torpedo Defence, MOD	1
Dr Mike Greening, MOD	1
Dr Jane Perkins, MOD	1
Dr Hatem Hmam, WSD	1
Electronics and Surveillance Research Laboratory	
Director, Electronics and Surveillance Research Laboratory	Doc Data Sht
Chief, Surveillance Systems Division	1
Chief, Electronic Warfare Division	1
Research Leader, Surveillance for Air Superiority, SSD	1
Dr John Percival, Head TSF, SSD	1

Dr John Whitrow, Head SSP, SSD	1
Ase Jakobsson, SSD	1
Authors	5

DSTO Research Library and Archives

Library Fishermans Bend	1
Library Maribyrnong	1
Library Salisbury	2
Australian Archives	1
Library, MOD, Pyrmont	Doc Data Sht
Library, MOD, HMAS Stirling	1
US Defense Technical Information Center	2
UK Defence Research Information Centre	2
Canada Defence Scientific Information Service	1
NZ Defence Information Centre	1
National Library of Australia	1

Capability Systems Staff

Director General Maritime Development	Doc Data Sht
Director General Land Development	1
Director General C3I Development	Doc Data Sht
Director General Aerospace Development	Doc Data Sht

Navy

SO(Science), Director of Naval Warfare, Maritime Headquarters Annex, Garden Island	Doc Data Sht

Army

ABCA Standardisation Officer, Puckapunyal	4
SO(Science), DJFHQ(L), MILPO, Enoggera, Queensland 4057	Doc Data Sht

Air Force

Intelligence Program

DGSTA, Defence Intelligence Organisation	1
Manager, Information Centre, Defence Intelligence Organisation	1

Acquisitions Program

Corporate Support Program

Library Manager, DLS, Canberra	1

UNIVERSITIES AND COLLEGES

Prof. Rob Evans, Dept EEE, The University of Melbourne	1

Australian Defence Force Academy Library	1
Head of Aerospace and Mechanical Engineering, ADFA	1
Deakin University Library, Serials Section (M List)	1
Hargrave Library, Monash University	Doc Data Sht
Librarian, Flinders University	1

OTHER ORGANISATIONS

NASA (Canberra)	1
AusInfo	1
State Library of South Australia	1
Parliamentary Library of South Australia	1

ABSTRACTING AND INFORMATION ORGANISATIONS

Library, Chemical Abstracts Reference Service	1
Engineering Societies Library, US	1
Materials Information, Cambridge Scientific Abstracts, US	1
Documents Librarian, The Center for Research Libraries, US	1

INFORMATION EXCHANGE AGREEMENT PARTNERS

Acquisitions Unit, Science Reference and Information Service, UK	1
Library – Exchange Desk, National Institute of Standards and Technology, US	1
National Aerospace Laboratory, Japan	1
National Aerospace Laboratory, Netherlands	1

SPARES

DSTO Salisbury Research Library	5

Total number of copies: 68

DEFENCE SCIENCE AND TECHNOLOGY ORGANISATION DOCUMENT CONTROL DATA	1. CAVEAT/PRIVACY MARKING

2. TITLE The Influence of Communication Bandwidth on Target Tracking with Angle Only Measurements from Two Platforms	3. SECURITY CLASSIFICATION Document (U) Title (U) Abstract (U)

4. AUTHORS Branko Ristic and Sanjeev Arulampalam	5. CORPORATE AUTHOR Electronics and Surveillance Research Laboratory PO Box 1500 Salisbury, South Australia, Australia 5108

6a. DSTO NUMBER DSTO–TR–1053	6b. AR NUMBER AR-011-595	6c. TYPE OF REPORT Technical Report	7. DOCUMENT DATE October 2000

8. FILE NUMBER B 9505-19-186	9. TASK NUMBER AIR 99/204	10. SPONSOR DACD	11. No OF PAGES 15	12. No OF REFS 9

13. URL on the World Wide Web http://www.dsto.defence.gov.au/corporate/ reports/DSTO–TR–1053.pdf	14. RELEASE AUTHORITY Chief, Surveillance Systems Division

15. SECONDARY RELEASE STATEMENT OF THIS DOCUMENT

Approved For Public Release

OVERSEAS ENQUIRIES OUTSIDE STATED LIMITATIONS SHOULD BE REFERRED THROUGH DOCUMENT EXCHANGE, PO BOX 1500, SALISBURY, SOUTH AUSTRALIA 5108

16. DELIBERATE ANNOUNCEMENT

No Limitations

17. CITATION IN OTHER DOCUMENTS

No Limitations

18. DEFTEST DESCRIPTORS

Target tracking angle-only measurements Cramer-Rao bound	Multiple sensors bandwidth limitation

19. ABSTRACT

A multi-platform angle-only tracking system combines the angular measurements from distributed networked sensors in order to estimate the full kinematic target state. This report investigates the effect of communication bandwidth on track quality in a system which receives angle-only measurements from two networked sensors installed on two airborne moving platforms. The investigation is based on the Cramér-Rao lower bound of the mean-square range error for the case considered. The bound is derived for recursive estimators with prior information and compared with two algorithms: (i) maximum likelihood estimation over a cumulative measurement set and (ii) extended Kalman filter with triangulated range estimates.